

**Single-metal-atom catalysts supported on graphdiyne catalyze CO
oxidation**

Chunyan Sun^a, Simin Huang^a, Mengru Huang^a, Xiangrui Zhang^a, Shusheng
Xu^a, Hui Wang^{b,c}, Yanyan Chen^{c,d}, Xue-Rong Shi^{a*}

^a School of Material Engineering, Shanghai University of Engineering Science,
Shanghai 201620, P.R. China

^b Key Laboratory of Biofuels, Qingdao Institute of Bioenergy and Bioprocess
Technology, Chinese Academy of Sciences, Qingdao 266101, P.R. China

^c University of the Chinese Academy of Sciences, Beijing 100049, P.R.
China

^d State Key Laboratory of Coal Conversion, Institute of Coal Chemistry,
Chinese Academy of Sciences, Taiyuan 030001, Shanxi, P.R. China

*Email: shixuer05@mails.ucas.ac.cn

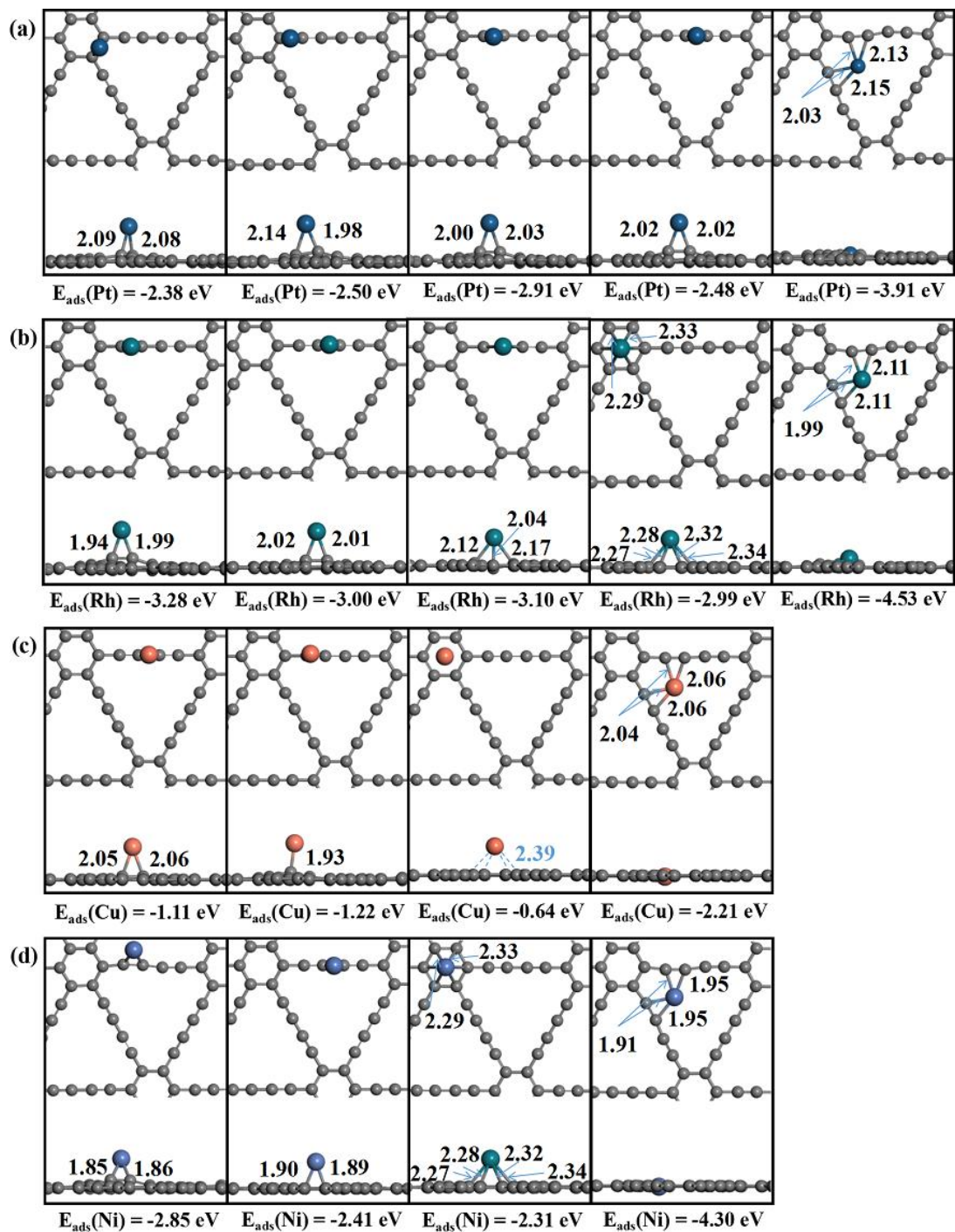


Figure S1. The obtained configuration and corresponding adsorption energy of single metal atom on GDY.

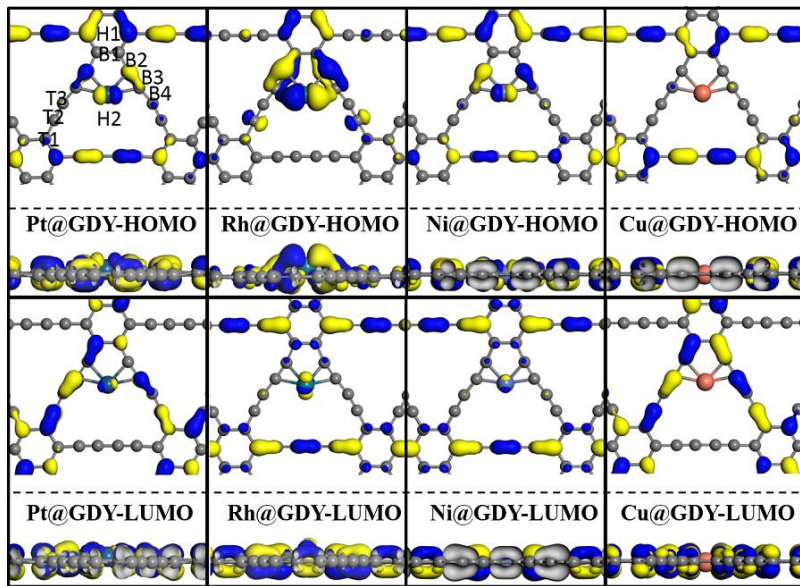


Figure S2. The absorption site for metal adsorption on GDY, and HOMO, LUMO of M@GDY.

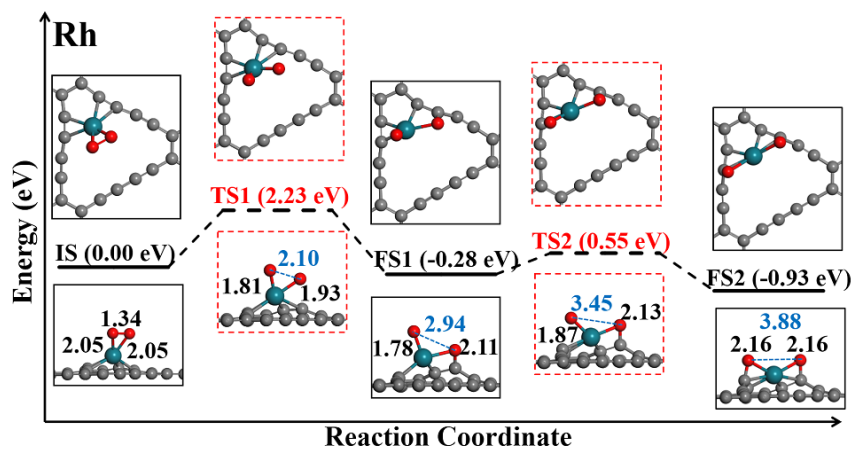


Figure S3. O_2 dissociation reaction pathway on Rh@GDY from the most stable IS to most stable product. For the other three systems, the reaction path from the most stable reactant to the most product presents only one TS, while for Rh@GDY it needs to cross two barriers.

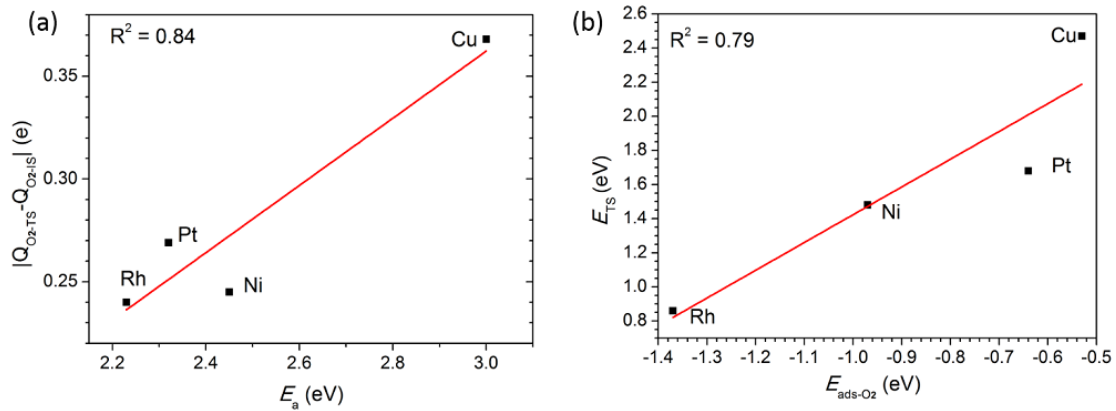


Figure S4. The linear fitting between (a) the O₂ dissociation barrier E_a and corresponding net change of Hirshfield charge of O₂ in TS and IS states $|Q_{O_2\text{-TS}} - Q_{O_2\text{-IS}}|$, and (b) the TS energy of O₂ dissociation relative to the initial gas state E_{TS} ($E_{\text{TS}} = E_{\text{total(TS)}} - E_{\text{total(M@GDY)}} - E_{\text{total(O}_2)}$) and O₂ adsorption energy $E_{\text{ads-O}_2}$ on M@GDY (M is labeled in the Figure).

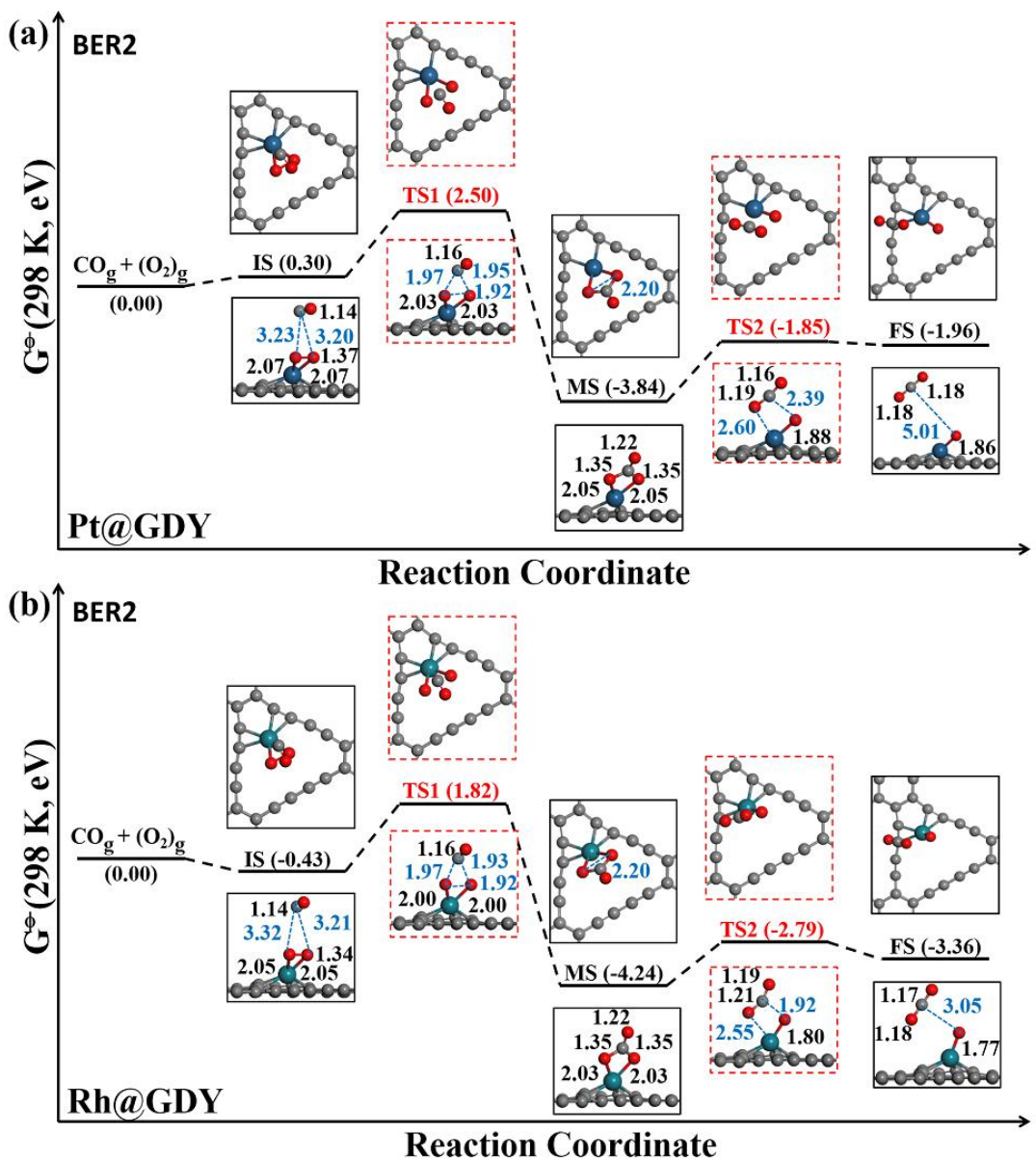


Figure S5. The configurations and standard Gibbs free energy profile at 298 K for the bi-molecular BER2 mechanism of CO oxidation on (a) Pt@GDY and (b) Rh@GDY. The energy value is provided in parentheses; the same below.

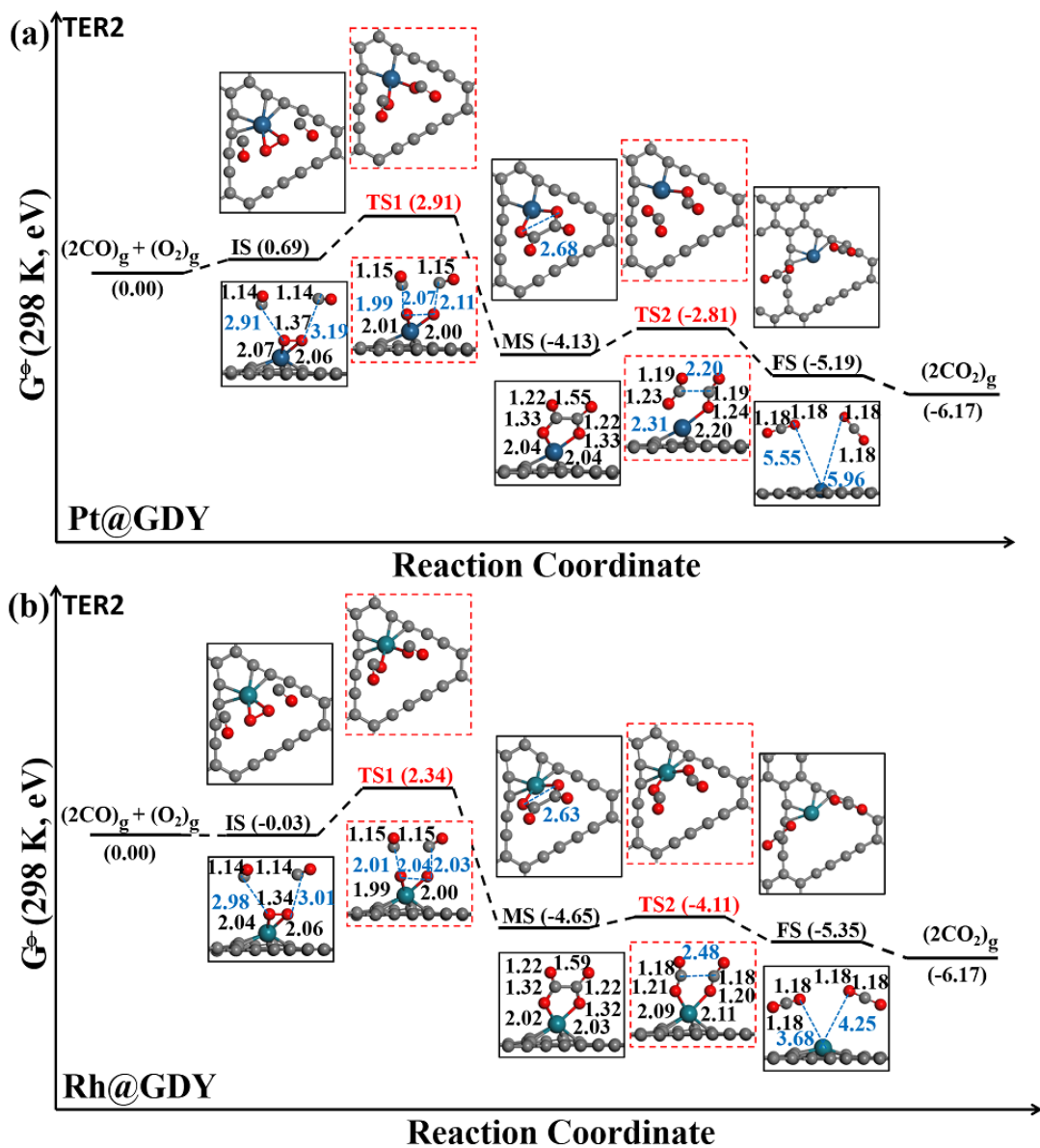


Figure S6. The configurations and standard Gibbs free energy profiles for the tri-molecular TER2 mechanism of CO oxidation on (a) Pt@GDY and (b) Rh@GDY.

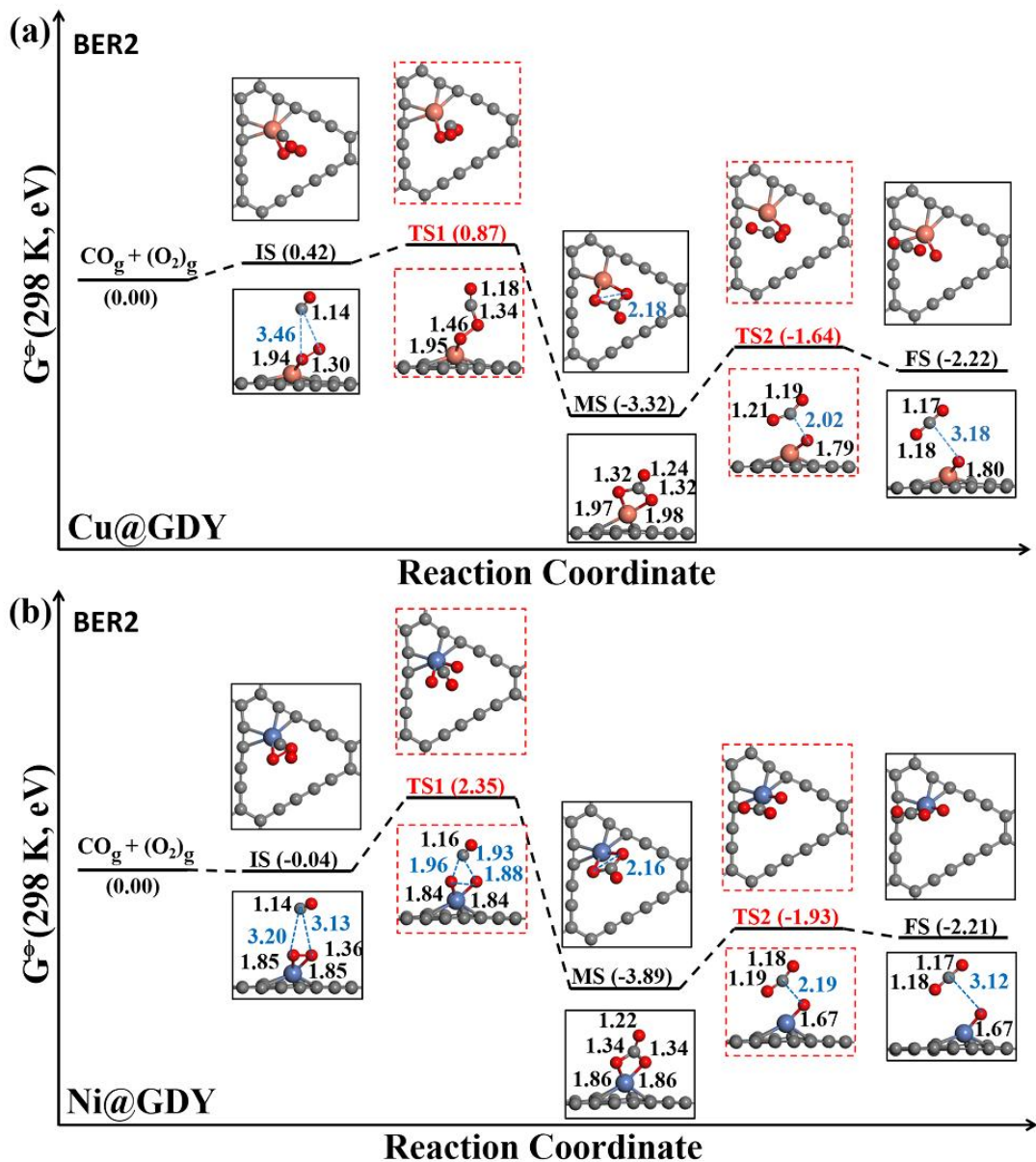


Figure S7. The configurations and standard Gibbs free energy profile at 298 K for the bi-molecular BER2 mechanism of CO oxidation on (a) Cu@GDY and (b) Ni@GDY. The energy value is provided in parentheses; the same below.

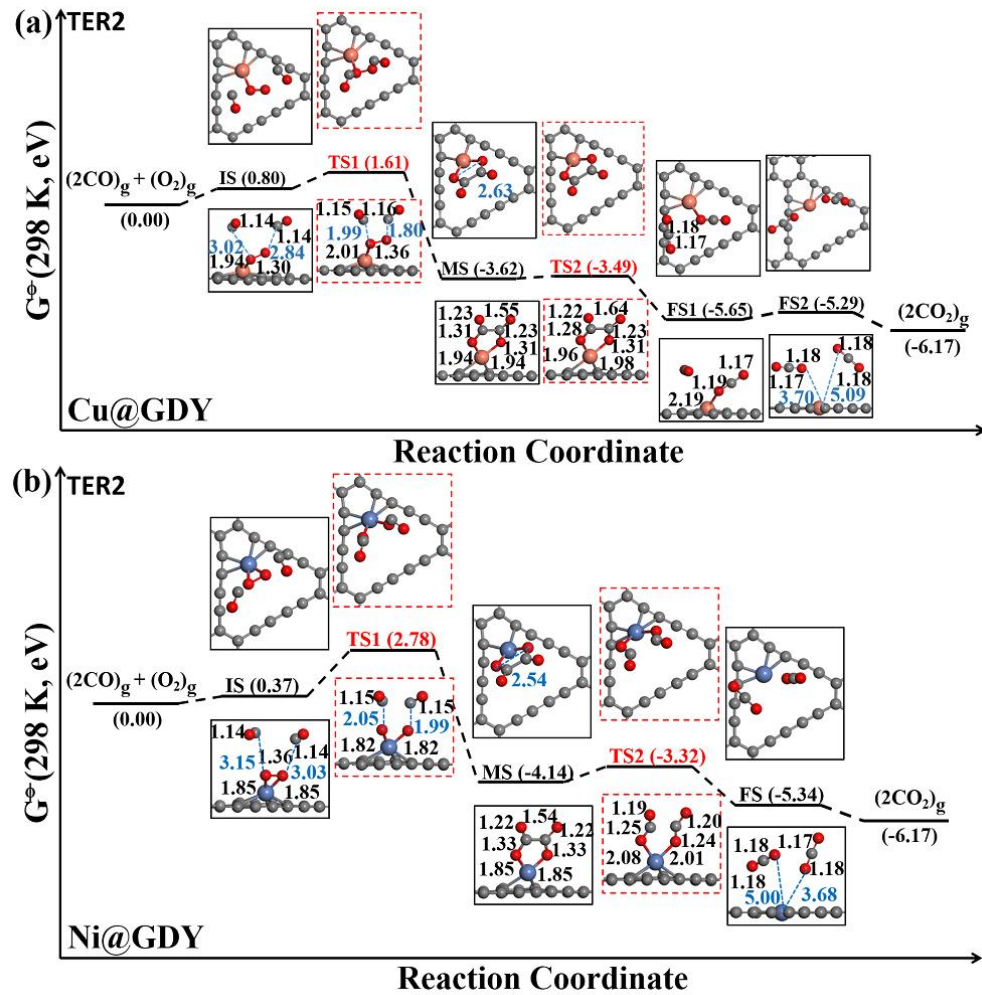


Figure S8. The configurations and standard Gibbs free energy profiles for the tri-molecular TER2 mechanism of CO oxidation on (a) Cu@GDY and (b) Ni@GDY.

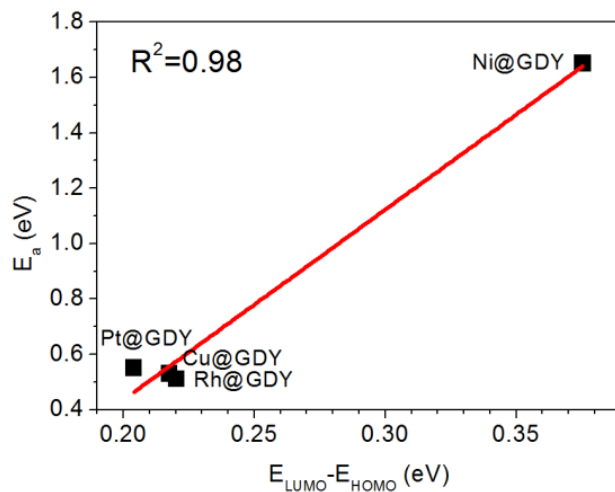


Figure S9. Correlation between E_a of rate-limiting steps and energy difference of LUMO and HOMO in IS for BLH on four M@GDY SACs.

Table S1. Summarization of adsorption and co-adsorption energies (eV).

	Pt@GDY	Rh@GDY	Cu@GDY	Ni@GDY
CO	-1.70	-1.61	-1.26	-1.68
O ₂	-0.64	-1.37	-0.53	-0.97
O	-2.84	-4.07	-2.64	-3.36
CO+O ₂	-1.27	-2.09	-1.16	-1.88
CO+CO	-1.86	-2.97	-1.78	-1.94
IS-TER1	-1.98	-3.09	-1.97	-2.04
IS-TER2	-0.89	-1.61	-0.78	-1.21

Table S2. Hirshfield charge |e|

	Pt			Rh			Ni			Cu		
	M	CO	O ₂									
M@GDY	0.24	--	--	0.26	--	--	0.15	--	--	0.44	--	--
BLH-IS	0.28	0.07	-0.19	0.25	0.03	-0.19	0.11	0.12	-0.18	0.33	0.09	-0.24
BLH-TS1	0.31	0.03	-0.27	0.31	0.03	-0.22	0.10	0.07	-0.17	0.32	-0.10	-0.24
BLH-MS	0.28	-0.11	-0.25	0.33	-0.09	-0.23	0.12	-0.02	-0.19	0.34	-0.08	-0.27
	M	CO ₂	O									
BLH-TS2	0.29	-0.21	-0.22	0.33	-0.17	-0.18	0.09	-0.02	-0.16	0.33	-0.03	-0.24
BLH-FS	0.35	0.00	-0.30	0.39	-0.01	-0.28	0.13	-0.01	-0.25	0.34	-0.02	-0.35